Dual-loop Model Extraction for Digital Predistortion of Wideband RF Power Amplifiers

Lei Guan, *Student Member*, *IEEE*, and Anding Zhu, *Member*, *IEEE*

***Abstract*— A dual-loop parameter characterization structure is proposed in order to improve the accuracy of the model extraction in digital predistortion systems. In this concept, a model reference loop is used in conjunction with a model inverse structure for fine tuning the model parameters. This model extraction process does not increase much of the complexity of system implementation but experimental results show that linearization performance can be significantly improved by employing the proposed structure for wideband RF power amplifiers.**

***Index Terms*— digital predistortion, dual loop, linearization, model extraction, power amplifier.**

I. Introduction

BECAUSE of its high flexibility, easy implementation and excellent performance, digital predistortion (DPD) has become one of the most preferred choices for linearizing RF power amplifiers (PAs) in modern wireless communication systems. In order to achieve the best linearization performance, DPD not only requires a compact and accurate behavioral model, but also needs a proper model extraction that is able to accurately find the model parameters.

Most existing DPD systems use either an indirect learning [1] or a *p*th-order post-inverse technique [2]. These model inverse structures are based on an assumption that the pre-inverse of the system is exactly the same as its post-inverse, so that we can use the same model for both the pre-inverse (DPD) and post-inverse. This assumption is only valid when the characteristics of the input and the output signals are very close. However, in a wideband system, due to strong nonlinear behavior of the PA, the signal characteristics can change significantly from the input to the output. Also, clipping effects due to PA saturation may cause the one-to-one mapping to be no longer applicable. As a result, the exact inverse response cannot be found for the signals at certain power levels. Furthermore, in a real system, the observed signals may be "corrupted" due to the limited bandwidth of the feedback loop and measurement noise in the data acquisition process. Therefore, it is very difficult to accurately extract parameters for the DPD by employing the model inverse structure, which often degrades the DPD performance.

As an alternative, a model reference structure was proposed in [3], in which coefficient optimization is achieved by comparing differences between the original input and the observed output of the PA directly, which eliminates the post-inverse process. However, this approach only works well if the residual distortion is small, otherwise the coefficient adaptation may diverge. In [4], a combined structure was proposed for enhancing the linearization performance for Doherty PAs. This cascade structure solves several problems when using the model inverse or the model reference structure separately. However, it contains two separate DPD branches/models, which significantly increases the complexity of system implementation.

In order to maximize linearization performance without excessively increasing complexity, we propose a new DPD structure in this letter, shown in Fig. 1, in which only one DPD model is employed but with two model extraction loops. The first loop is based on the *p*th-order post-inverse for coarse model extraction while the second loop uses the model reference structure for fine tuning. This structure does not greatly increase DPD system complexity, but significantly improves the system performance.

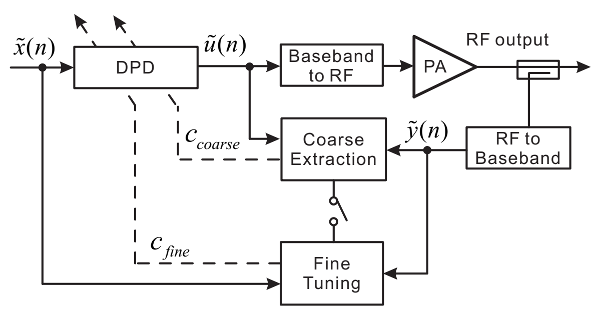

Fig.1 Proposed DPD structure with dual-loop model extraction.

II. Dual-loop Parameter Extraction

The DPD model employed is derived from the first-order truncated dynamic deviation reduction-based Volterra model [2], which can be written as,

$$\begin{aligned}\tilde{u}(n) &= \sum_{k=0}^{\frac{P-1}{2}} \sum_{m=0}^{M} \tilde{g}_{2k+1,1}(m)\left|\tilde{x}(n)\right|^{2k} \tilde{x}(n-m) \\ &+ \sum_{k=1}^{\frac{P-1}{2}} \sum_{m=1}^{M} \tilde{g}_{2k+1,2}(m)\left|\tilde{x}(n)\right|^{2(k-1)} \tilde{x}^{2}(n)\tilde{x}^{*}(n-m)\end{aligned} \tag{1}$$

Manuscript received December 22, 2010; resubmitted April 11, 2011; revised June 29, 2011; accepted July 6, 2011. This work was supported by the Science Foundation Ireland under the Principal Investigator Award scheme.

The authors are with the School of Electrical, Electronic and Communications Engineering, University College Dublin, Dublin 4, Ireland (e-mail: lei.guan@ucd.ie; anding.zhu@ucd.ie).

where $\tilde{x}(n)$ and $\tilde{u}(n)$ are the baseband input and output, respectively. $\tilde{g}_{2k+1,j}(m)$ is the coefficient. P and M are the nonlinear order and memory length, respectively.

A. Coarse Extraction

In the coarse extraction loop, the adaptive *p*th-order post-inverse is used [2]. During the model extraction process, the feedback signal, i.e., the output of the PA, $\tilde{y}(n)$, is used as the input to the DPD, while the predistorted output signal $\tilde{u}(n)$ is the expected output. The least squares (LS) algorithm is used for model extraction, which can be described as follows,

$$C_{coarse(i)} = (Y_{(i-1)}^{H} Y_{(i-1)})^{-1} Y_{(i-1)}^{H} U_{(i-1)} \tag{2}$$

where $C_{coarse(i)}$ represents the parameter vector of the predistorter, which contains all of the unknown coefficients $\tilde{g}_{2k+1,j}(m)$ in the DPD model. The subscript of $(\cdot)_{(i)}$ indicates the *i*th iteration and $(\cdot)^{H}$ represents Hermitian transpose. The vector $U_{(i-1)}$ represents the DPD output vector in the previous iteration. The matrix $Y_{(i-1)}$ includes all of the linear and product terms, such as $\tilde{y}(n)$, $\tilde{y}(n-m)$, …, $\left|\tilde{y}(n)\right|^{2}\tilde{y}(n)$, …, appearing in the input of the model in the previous iteration for $m = M+1,\cdots,L$, where L is the total length of the data used. For the first iteration, the DPD block is bypassed, so that the initial DPD output $\tilde{u}(n)$ is identical to the original input $\tilde{x}(n)$. From the second iteration, the coefficients are calculated according to (2), and the new DPD output can be derived from

$$U_{(i)} = X_{(i)} C_{coarse(i)} \tag{3}$$

The matrix $X_{(i)}$ contains the linear and product terms of the current input in a similar form to the matrix $Y_{(i)}$. The iteration stops when a minimum error value is reached.

This model inverse structure can effectively extract the DPD parameters and thus compensate for distortion induced by PA nonlinearities. However, some errors may still remain after the model extraction process, even if the DPD model itself can perfectly represent the inverse of the PA behavior. In other words, this structure cannot completely extract the parameters of the DPD. This is because that, in the first iteration, the (un-linearized) PA output is very different from the original input due to the nonlinear amplification processing by the PA, which causes the post-inverse (the mapping from the output to the input of the PA) to be different from the pre-inverse (digital predistortion). This error affects the system performance in an accumulative way since the signal predistorted by the "inaccurate" DPD model is used as the expected output in the following iterations. Therefore, although the output of the PA is approaching the original input after several iterations, there are still some deterministic errors between these two signals, which cannot be corrected due to the inherent defects of the model extraction process.

B. Fine Tuning

In order to compensate for the residual error in the coarse model extraction, we introduce another parallel branch based on the model reference structure [3], to finely tune the coefficients of the DPD. Since the residual error between the original input $\tilde{x}(n)$ and the linearized output $\tilde{y}(n)$ becomes very small after the coarse predistortion, this output error can be made approximately equal to the expected error at the input of the PA, namely,

$$\tilde{e}_{(n)} = G^{-1}\left(\tilde{y}_{(n)} - \tilde{x}_{(n)}\right) \approx \tilde{y}_{(n)} - \tilde{x}_{(n)} \tag{4}$$

where $G^{-1}(\cdot)$ is the inverse transfer function of the PA. This error should be subtracted from the output of the DPD, so that the error at the PA output can be removed. To produce this error signal, we must extract the deviated coefficients using the equation below,

$$C_{fine(i)} = (X_{(i-1)}^{H} X_{(i-1)})^{-1} X_{(i-1)}^{H} E_{(i-1)} \tag{5}$$

where $C_{fine(i)}$ is the deviated coefficients vector for the DPD and $X_{(i-1)}$ is the input matrix formed from the original input signal $\tilde{x}(n)$ in a similar form to the matrix $Y_{(i-1)}$ in (2). $E_{(i-1)}$ is the error vector formed from $\tilde{e}_{(n)}$. The deviated coefficients are then subtracted from the existing coefficients,

$$C_{(i)} = C_{(i-1)} - \lambda C_{fine(i-1)} \quad (0 < \lambda \le 1) \tag{6}$$

where λ represents the sensitivity factor, which is used for controlling the convergence speed. In our tests, $\lambda \approx 0.707$. The initial value of $C_{(i-1)}$ should be copied from the coarse model extraction branch, i.e., $C_{(0)} = C_{coarse(i)}$. The final DPD output can be expressed as

$$U_{(i)} = X_{(i)} C_{(i)} \tag{7}$$

Compared to the combined structure in [4], this dual-loop model extraction does not increase much of the implementation complexity or cost since we still use the same DPD model and the same LS algorithm in (2) and (5). The only difference is that we change the reference signal from the DPD output to the original input, which is already available in the real system. However, this extra fine tuning process can effectively find a properly deviated coefficient adjustment that can be used for further optimization of the model parameters to reduce model extraction errors and thus improve DPD performance.

III. Experimental Results

In order to validate the performance of the proposed DPD parameter extraction structure, we tested a LDMOS Doherty amplifier operated at 2.14 GHz and excited with a 40 MHz 8-carrier WCDMA signal with an average output power of 45 dBm. The test bench was set up to be similar to that in [2], where a baseband I/Q complex signal was created in MATLAB, and fed to an RF board to modulate and up-convert to the RF frequency, and then sent to the PA. In the output, the RF signal was down-converted and demodulated to baseband. The baseband I/Q data sampling rate was 184.32 M samples/second.

TABLE I
PERFORMANCE OF THE DPD FOR AN 8-CARRIER WCDMA SIGNAL

No	Iterations	NRMSE	ACPR1 (dBc)		ACPR2 (dBc)	
			-5MHz	+5MHz	-10MHz	+10MHz
1	Without DPD	10.77%	-26.6	-24.6	-27.2	-25.8
2	CE 1	3.00%	-37.4	-36.5	-37.8	-37.9
3	CE 2	1.18%	-46.6	-45.9	-47.0	-47.3
4	CE 3	0.72%	-50.5	-49.7	-50.9	-50.8
5	FT 1	0.52%	-53.8	-53.3	-53.4	-54.1
6	FT 2	0.42%	-56.8	-55.8	-56.4	-56.8
7	FT 3	0.39%	-57.5	-56.9	-57.8	-57.9

CE: Coarse Extraction; FT: Fine tuning.

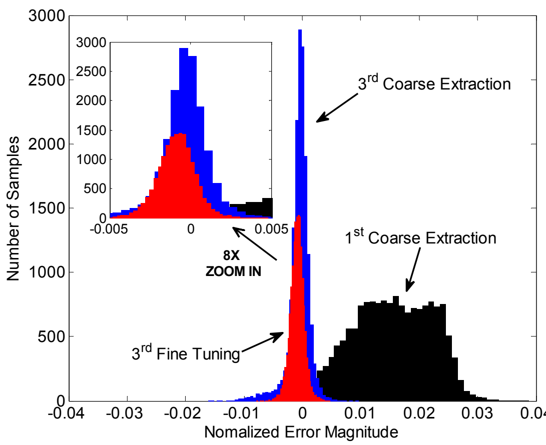

Fig. 2 The amplitude distribution of the error signal between the linearized output and the original input.

Table I gives the NRMSE (normalized root mean square error) [2] and ACPR (adjacent channel power ratio) performance for the test signal. With the coarse extraction, after three iterations, the ACPRs reached around -50 dBc and no further improvement can be made. However, after the fine tuning process was applied, more than 7 dB of further (over 30%) improvement was achieved; and in total more than 30 dB ACPR improvement was achieved. NRMSE was also improved from 0.72% to 0.39% with the fine tuning.

Further improvement made by the fine tuning means that there are still deterministic errors existing in the model parameters, which should be corrected but cannot be removed by the model inverse structure due to its inherent imperfection. It can be further verified by plotting the statistical distribution of the error signal, shown in Fig. 2. After the first iteration, the residual error could follow a random distribution, but when the system is converged, only random noise and measurement errors will remain, if a proper linearization procedure is applied. The "ideal" residual error must therefore follow a Gaussian distribution in the end. However, from Fig. 2, we can see that a Gaussian distribution only can be reached after fine tuning.

Finally, the frequency spectra of the PA output are shown in Fig. 3, and the AM/AM and AM/PM plots are shown in Fig.4, where we can see that, nonlinear distortion consisting of both static nonlinearities and memory effects, induced by the PA, are almost completely removed after the dual-loop predistortion.

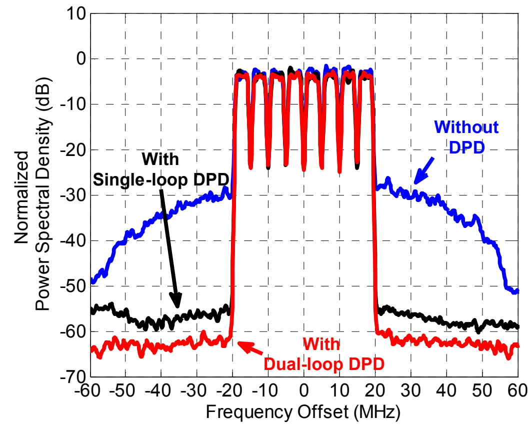

Fig. 3 Output spectra for an 8-carrier WCDMA signal with and without DPD.

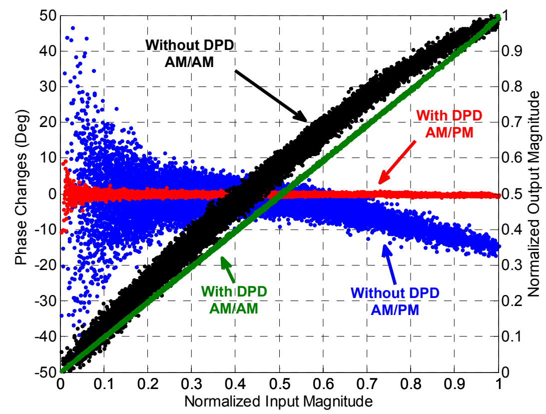

Fig. 4 AM/AM and AM/PM plots for an 8-carrier WCDMA signal with and without DPD.

IV. CONCLUSION

In this letter, in order to improve the accuracy of DPD model extraction, we propose a dual-loop parameter characterization structure, which uses the model inverse structure for coarse extraction and then employs a model reference loop to finely tune the values of the parameters in order to remove residual errors. Experimental results have demonstrated that the proposed model extraction structure can significantly improve DPD performance without greatly increasing the implementation complexity or cost.

REFERENCES

[1] L. Ding, G. T. Zhou, D. R. Morgan, Z. Ma, J. S. Kenney, J. Kim, and C. R. Giardina, "A robust digital baseband predistorter constructed using memory polynomials," *IEEE Trans. Commun.*, vol. 52, no. 1, pp. 159 – 165, Jan. 2004.

[2] A. Zhu, P. J. Draxler, J. J Yan, T. J. Brazil, D. F. Kinball, and P. M. Asbeck, "Open-loop digital predistorter for RF power amplifiers using dynamic deviation reduction-based Volterra series," *IEEE Trans. Microw. Theory Tech*, vol. 56, no. 7, pp. 1524-1534, Jul. 2008.

[3] P. Draxler, J. Deng, D. Kimball, I. Langmore, and P.M. Asbeck, "Memory effect evaluation and predistortion of power amplifiers," in *IEEE MTT-S Int. Microw. Symp. Dig.*, Long Beach, CA, Jun. 2005, pp. 1549–1552.

[4] R. N. Braithwaite, "An improved Doherty amplifier using cascaded digital predistortion and digital gate voltage enhancement", *IEEE Trans. Microw. Theory Tech*, vol. 57, no. 12, pp. 3118-3126, Dec. 2009.